DOI: 10.1002/chem.201000684

Fabrication of a Biocompatible and Conductive Platform Based on a Single-Stranded DNA/Graphene Nanocomposite for Direct Electrochemistry and Electrocatalysis

Qian Zhang,[a, b] Yun Qiao,[a, b] Fei Hao,[a, b] Ling Zhang,[d] Shuyao Wu,[a, b] Ying Li,[b] Jinghong Li,*[c] and Xi-Ming Song*[a, b]

Abstract: A novel electrochemical platform was designed by combining the biocompatibility of single-stranded DNA (ss-DNA) and the excellent conductivity of graphene (GP). This nanocomposite (denoted as ss-DNA/GP) was first used as an electrode material for the immobilization and biosensing of redox enzymes. On the basis of electrostatic interactions, horseradish peroxidase (HRP) self-assembled with ss-DNA/GP on the surface of a glassy carbon (GC) electrode to form an HRP/ss-DNA/GP/GC electrode. UV/Vis and FTIR spectra were used to monitor the assembly process and indicated that the immobilized HRP on the ss-DNA/GP matrix retained its native structure well. A pair of stable and well-defined redox peaks of HRP with a formal potential of about −0.26 V (vs. Ag/AgCl) in a pH 7.0 phosphate buffer solution were obtained at the HRP/ss-DNA/GP/GC electrode; this demonstrates direct electron transfer between the immobilized HRP and the electrode. In addition, the modified electrode showed good electrocatalytic performance towards H_2O_2 with high sensitivity, wide linear range, and good stability. Accordingly, the ss-DNA/GP nanocomposite provides a novel and efficient platform for the immobilized redox enzyme to realize direct electrochemistry and has a promising application in the fabrication of third-generation electrochemical biosensors.

Keywords: DNA · electrocatalysis · electrochemistry · graphene · nanocomposite

Introduction

Biocompatible nanocomposites have drawn increasing attention owing to their promising properties and compatibility with bioactive proteins and enzymes. These composites, which integrate natural biomolecules, hydrogels, or biopolymers with nanomaterials, possess superior properties to those of the independent components and have found great potential for applications in various fields, especially in the field of bioelectrochemistry.[1] It has been proven that such nanocomposites could provide favorable microenvironments for redox proteins and enzymes to realize direct electrochemistry and could be used in the construction of excellent electrochemical biosensors. So far, various biocompatible nanocomposites have been utilized for the fabrication of biosensors.[2] Among them, carbon-based biocomposites have attracted considerable attention because of their unique electronic and structural characteristics.[3] On the basis of these attractive properties, carbon-based biocomposites could act as effective supports for the immobilization

[a] Dr. Q. Zhang,[+] Y. Qiao,[+] F. Hao, S. Wu, Prof. X.-M. Song
Liaoning Provincial Key Laboratory for Green Synthesis and Preparative Chemistry of Advanced Materials
Liaoning University, Shenyang 110036 (China)
Fax: (+86) 24-6220-2378
E-mail: songlab@lnu.edu.cn

[b] Dr. Q. Zhang,[+] Y. Qiao,[+] F. Hao, S. Wu, Y. Li, Prof. X.-M. Song
College of Chemistry, Liaoning University
Shenyang 110036 (China)

[c] Prof. J. Li
Department of Chemistry
Key Laboratory of Bioorganic Phosphorus Chemistry & Chemical Biology
Tsinghua University, Beijing 100084 (China)
Fax: (+86) 526-2243
E-mail: jhli@mail.tsinghua.edu.cn

[d] Dr. L. Zhang
College of Chemistry and Life Science
Shenyang Normal University, Shenyang 110034 (China)

[+] These authors contributed equally to this paper.

of redox enzymes and for the fabrication of biosensors with improved electrochemical performance.

Graphene (GP), a two-dimensional carbon nanomaterial, has attracted great interest due to its unique structure and properties, such as large specific surface area, high thermal conductivity, and extraordinary electronic transport properties.[4] GP has gained increasing attention for a variety of applications because of these exciting properties.[5] At present, more and more attempts have been made for the application of GP in bioelectrochemistry.[6] It has been found that GP is a promising material for the fabrication of electrochemical biosensors, and it has shown great potential to promote the electron transfer of redox enzymes on electrodes.[7] For example, Shan et al. constructed a polyvinylpyrrolidone-protected GP/polyethylenimine-functionalized ionic liquid/glucose oxidase (GOD) electrochemical biosensor based on the direct electrochemistry of GOD.[8] Also using GOD as a model enzyme, Chen and co-workers fabricated a GOD/GP/Nafion composite film modified electrode to realize the direct electrochemistry of GOD.[9] Compared with other carbon-based nanomaterials such as carbon nanotubes (CNTs), GP possesses some advantages for the fabrication of electrochemical biosensors, such as its low cost, increased surface area, and specific nanosheet structure. However, the utilization of GP, especially in a biocompatible form, to construct biosensors is still limited.

Deoxyribonucleic acid (DNA), which is a well-known natural biological macromolecule, has gained increasing attention in the field of biotechnology.[10] Recently, the combination of DNA with carbon-based nanomaterials such as CNTs for the development of novel biomaterials and devices has attracted great attention in the field of DNA transporters,[11] field-effect transistors,[12] and gene therapy.[13] Such biocompatible nanocomposites are also of interest for applications in enzyme immobilization and direct electrochemistry.[14] It has been found that the bioactivities of metalloproteins could be greatly enhanced by being immobilized together with DNA on the surface of a solid matrix.[15] Compared with independent carbon nanomaterials or DNA-based enzyme electrodes, such nanocomposite-based enzyme electrode therefore often exhibit better electrochemical performance.[16] For example, our previous study showed that the utilization of DNA/CNT nanocomposites as the electrode material could greatly enhance the faradic responses and bioelectrochemical catalytic activities of the enzyme electrode.[17] Therefore, it is meaningful to exploit novel DNA-based nanocomposites for electrochemical biosensing applications. Recently, it has been found that single-stranded DNA (ss-DNA) could form a stable nanocomposite with GP through π–π stacking interactions.[18,19] Owing to such efficient combination, the resulting ss-DNA/GP nanocomposite is endowed with the excellent properties of the two independent components, such as the biocompatiblity of DNA and the outstanding electronic properties of GP. Furthermore, the existence of DNA on GP not only assisted the dispersion of GP in aqueous solution but also made it exhibit a negative charge, which is favorable for the further immobilization of biomolecules through self-assembly.

Herein, by taking the advantages of ss-DNA and GP, we propose a novel design for the fabrication of an enzyme electrode to realize direct electrochemistry. Horseradish peroxidase (HRP) was immobilized on ss-DNA/GP through a self-assembly method to form a multicomponent nanocomposite on a glassy carbon (GC) electrode (Figure 1). The experimental results demonstrated that such an electrochemical platform not only preserved the native structure of the immobilized enzyme but also exhibited good electron-transfer properties for HRP. Meanwhile, the as-prepared HRP/ss-DNA/GP/GC electrode exhibited good analytical performance towards the quantification of hydrogen peroxide, with a wide linear range, good reproducibility, and long-term stability. Therefore, this kind of biocomposite film offers a promising platform for the development of novel electrochemical biosensors.

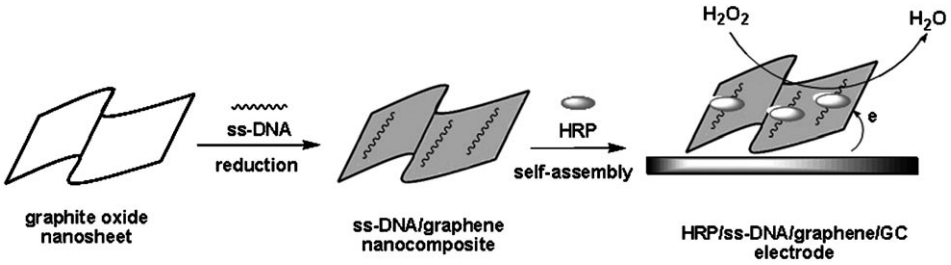

Figure 1. Scheme of fabrication of the HRP/ss-DNA/GP/GC electrode and the direct electron transfer between immobilized HRP and the GC electrode.

Results and Discussion

Characterization of the ss-DNA/GP nanocomposite: The morphological characters of the as-synthesized ss-DNA/GP nanocomposite were obtained by transmission electron microscopy (TEM). Figure 2a presents a typical TEM image of ss-DNA/GP. As shown, the ss-DNA/GP was in the form of ultrathin sheets from 500 nm to 1 μm in size. Furthermore, it is obvious that there is some corrugation and scrolling on the edge of the nanosheet. Figure 2b and c show photographs of unmodified GP and ss-DNA/GP, respectively, dispersed in water. It can be observed from Figure 2b that the unmodified GP could not be dispersed in water. By contrast, ss-DNA/GP could be readily dispersed in water to form a black suspension, which indicated that the nanocom-

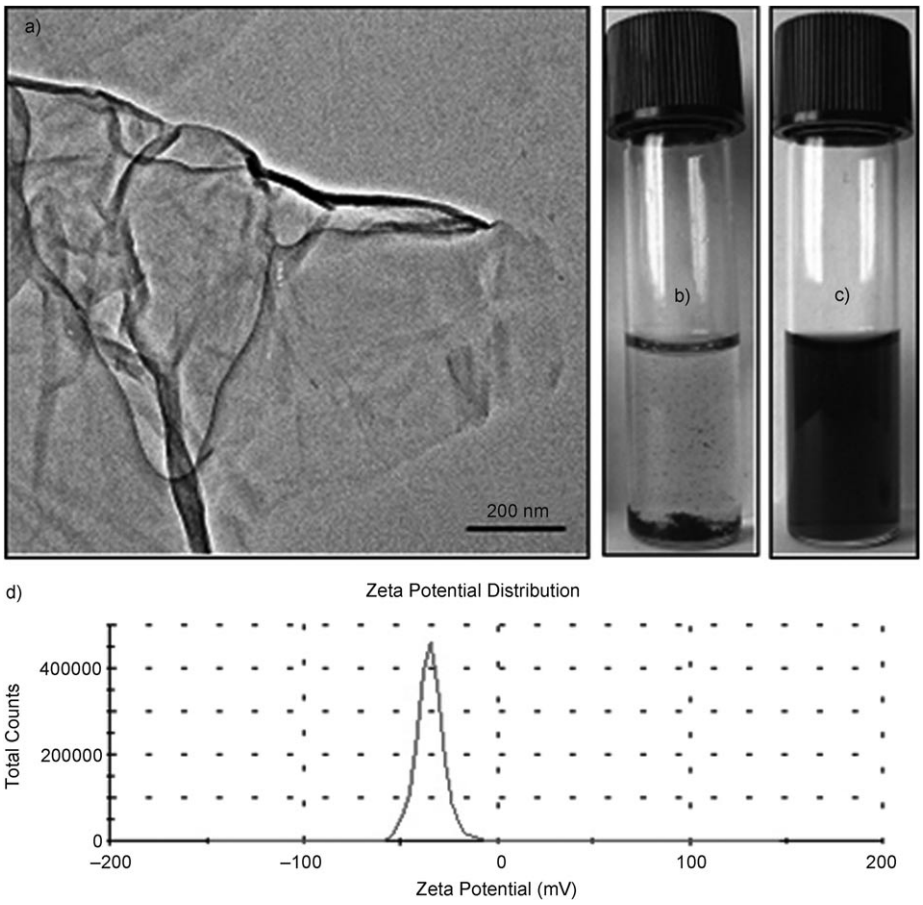

Figure 2. a) TEM image of ss-DNA/GP, b,c) photographs of unmodified GP (b) and ss-DNA/GP (c) in water, and d) zeta-potential data of ss-DNA/GP in phosphate buffer solution (PBS) at pH 5.0.

posite was highly hydrophilic. This homogeneous suspension was stable even after storage for several months. Figure 2d shows the zeta-potential data of ss-DNA/GP in PBS at pH 5.0. The ss-DNA/GP nanocomposite possessed a strongly negative charge of nearly −38 mV at pH 5.0; this result is similar to that with ss-DNA (−41 mV) under the same conditions. Such a negative charge was important for the stable dispersion of ss-DNA/GP in aqueous solution because it could form electrostatic hindrance around the GP nanosheet to prevent aggregation.

Fabrication of HRP/ss-DNA/GP/GC electrode: The fabrication of the HRP/ss-DNA/GP/GC electrode is depicted in Figure 1. Firstly, hydrophilic graphite oxide (GO) aqueous suspension was obtained through the method of Hummers and Offeman.[20] The GO was then reduced by hydrazine in the presence of ss-DNA. Due to the π–π stacking interactions between purine and pyrimidine bases of the DNA molecules and GP, ss-DNA could adsorb on the surface of the GP to form an ss-DNA/GP nanocomposite during the chemical reduction procedure. The existence of ss-DNA on GP not only provided the nanocomposite biocompatibility and water solubility but also endowed the nanocomposite with a negative charge in aqueous solution. HRP is an amphoteric protein (the pH value at isoelectric point is 8.9), so it exhibits a positive charge at pH values below its isoelectric point. When the electrode based on ss-DNA/GP was immersed in an aqueous solution of HRP at pH 5.0, the enzyme molecule could adsorb onto the surface of the ss-DNA/GP through electrostatic interactions to form HRP/ss-DNA/GP nanocomposites on the GC electrode. It is known that electrostatic interactions play an important role during the self-assembly process between the enzyme and nanomaterials, which allows the enzyme to immobilize on the nanomatrix under mild conditions; thus, the native structure and bioactivity of the immobilized enzyme were retained.[17]

UV/Vis and FTIR spectroscopic analysis of the HRP/ss-DNA/GP composite: UV/Vis absorption spectroscopy was used to monitor the self-assembly process of the HRP/ss-DNA/GP nanocomposite (Figure 3). The UV/Vis spectra of free HRP

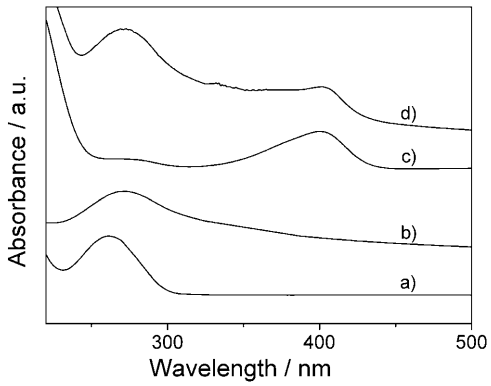

Figure 3. UV/Vis absorption spectra of a) ss-DNA, b) ss-DNA/GP, c) HRP, and d) HRP/ss-DNA/GP in PBS at pH 7.0.

(line c in Figure 3) and ss-DNA (line a in Figure 3) in aqueous solution exhibited strong absorbances at 402 and 260 nm, respectively. The adsorption peak of ss-DNA/GP appeared at 272 nm (line b in Figure 3). As previously known, the exfoliated GP suspension in water displayed a strong absorption band at around 270 nm.[21] After ss-DNA adsorbed onto GP, this adsorption peak was covered by the adsorption peak of the ss-DNA located at around 260 nm; thus, the adsorption peak of the ss-DNA/GP nanocomposite

appeared at 266 nm. Therefore, these results demonstrated the chemisorption of ss-DNA on the GP nanosheet. The ss-DNA/GP was further electrostatically interacted with HRP. It is evident that a peak appeared at 402 nm in the spectrum of the HRP/ss-DNA/GP sample (line d in Figure 3), which was due to the alternative absorption of HRP on ss-DNA/GP. The Soret band of HRP at 402 nm was unaffected during the self-assembly process, which suggests that the immobilized HRP maintained its native structure.

Figure 4 shows the FTIR spectra of GO, ss-DNA/GP, HRP, ss-DNA, and HRP/ss-DNA/GP. It could be observed that the FTIR spectrum of ss-DNA/GP (line b in Figure 4)

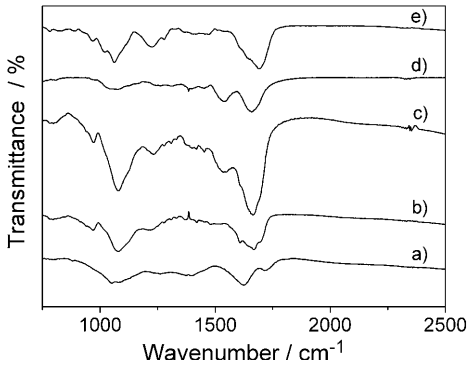

Figure 4. FTIR spectra of a) GO, b) ss-DNA/GP, c) HRP/ss-DNA/GP, d) HRP, and e) ss-DNA.

is quite different from that of GO (line a in Figure 4). Moreover, it is obvious that the FTIR spectrum of ss-DNA/GP exhibited a strong adsorption band at 1700 cm^{-1}. This adsorption band was attributable to the base-pair infrared absorbance of ss-DNA, which was similar to that observed with free ss-DNA (line e in Figure 4) and therefore indicates the existence of ss-DNA on the GP nanocomposite. After ss-DNA/GP further interacted with HRP, it could be seen that the FTIR spectrum of the HRP/ss-DNA/GP nanocomposite (line c in Figure 4) exhibited the amide I (1654 cm^{-1}) and II (1545 cm^{-1}) bands of the immobilized enzyme. These adsorption bands were all essentially the same as those of the native HRP (line d in Figure 4), which demonstrated that the secondary structures of the immobilized enzyme were undisturbed. In addition, it could also be observed that the amide I band of HRP/ss-DNA/GP was broader than that of the native HRP, which was due to overlap of the base-pair band of DNA at 1700 cm^{-1} and the amide I band of HRP at 1654 cm^{-1}. On the basis of the above-mentioned results, ss-DNA/GP could be a good matrix for the immobilization of enzymes because of its excellent biocompability.

Electrochemical properties of the HRP/ss-DNA/GP/GC electrode: Figure 5 A displays typical cyclic voltammograms (CVs) for HRP/GC, ss-DNA/GP/GC, and HRP/ss-DNA/GP/GC electrodes in 0.1 M PBS (pH 7.0) over the potential range from 0.2 to −0.8 V at a scan rate of 200 $mV s^{-1}$ (lines a–c, respectively). No redox peak was observed at the

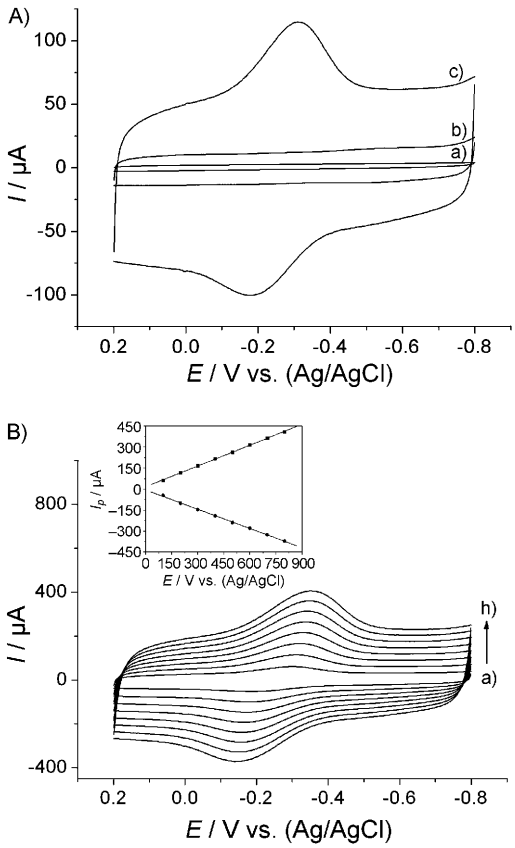

Figure 5. A) Cyclic voltammograms of a) HRP/GC, b) ss-DNA/GP/GC, and c) HRP/ss-DNA/GP/GC electrodes in 0.1 M PBS (pH 7.0). Scan rate: 200 $mV s^{-1}$. B) Cyclic voltammograms of the HRP/ss-DNA/GP/GC electrode at scan rates of 100, 200, 300, 400, 500, 600, and 700 $mV s^{-1}$ in 0.1 M PBS (pH 7.0), respectively. Inset: plots of the oxidation peak current (●) and reduction peak current (■) versus the scan rate for the HRP/ss-DNA/GP/GC electrode.

HRP/GC electrode (line a in Figure 5 A), possibly due to the unfavorable orientation or denaturation of HRP molecules on the bare GC electrode surface. There was also no redox peak observed at the ss-DNA/GP/GC electrode (line b in Figure 5 A), which suggests that the ss-DNA/GP nanocomposite was not electroactive in the potential range. By comparison, a couple of well-defined peaks were observed for the HRP/ss-DNA/GP/GC electrode (line c in Figure 5 A); these peaks indicated direct electron transfer for the HRP Fe^{III}/Fe^{II} redox pair at the HRP/ss-DNA/GP/GC electrode. The cathodic and anodic peak potentials were at −0.32 and −0.20 V, respectively. The formal potential (E_p), calculated from the average value of the cathodic and anodic peak potentials, was −0.26 V, which was consistent with previous literature.[22] This result demonstrated that the ss-DNA/GP nanocomposite played an important role in facilitating direct electron transfer between HRP and the GC electrode. Being a nanocomposite, ss-DNA/GP combined the advantages of both components, such as the good biocompatibility of DNA and the excellent electron-transport properties and large surface area of GP, which could provide a conductive and favorable microenvironment for the immo-

bilized HRP to realize direct electrochemistry. Moreover, it should be noted that a largely reduced interfacial capacitance was observed at the HRP/ss-DNA/GP/GC electrode, which was quite different from many other nanomaterial-based enzyme electrodes.[23,24] The reduced interfacial capacitance was possibly contributable to the unique structure of the ss-DNA/GP nanocomposite.

The influence of scan rate on the response of the immobilized HRP is shown in Figure 5B. It can be observed that both the reduction and oxidation peak currents (I_p) were increasing linearly with scan rates from 100 to 700 mV s^{-1}, which indicates surface-controlled processes of the electrode reaction. Moreover, integration of the reduction peaks at different scan rates gave nearly constant charge values. According to Faraday's law, $Q = nFA\Gamma^*$, in which F is the Faraday constant, Γ^* represents the surface concentration of electroactive HRP, Q can be calculated by integrating the reduction peak of HRP, n stands for the electron-transfer number, and A represents the area of the electrode surface, which herein was taken as the geometric area of the GC electrode (0.07 cm^2). The surface concentration of electroactive HRP (Γ^*) at the HRP/ss-DNA/GP/GC electrode was calculated to be 9.48×10^{-9} mol cm^{-2}, which is much higher than the reported value for HRP in other immobilized matrices, such as DNA (5.1×10^{-11} mol cm^{-2}),[22] DNA/single-walled CNTs (SWCNTs; 1.2×10^{-10} mol cm^{-2}),[16] cetyltrimethylammonium bromide/SWCNTs (8.83×10^{-10} mol cm^{-2}),[25] carbon black (1.83×10^{-10} mol cm^{-2}),[26] gold nanoparticles/silk fibroin (1.8×10^{-9} mol cm^{-2}),[27] hexagonal mesoporous silicas (HMS) (9.4×10^{-10} mol cm^{-2}),[28] and the ionic liquid 1-butyl-3-methylimidazolium tetrafluoroborate (1.03×10^{-10} mol cm^{-2}).[29] This result indicated that the ss-DNA/GP nanocomposite possessed a high enzyme-loading ability, which can be attributed to the large specific surface area and the crumpled nanosheet structure of the nanocomposite. Moreover, the theoretical monolayer coverage for HRP is about 2.0×10^{-11} mol cm^{-2}.[23] The value obtained in our experiment is much higher than that of the theoretical monolayer coverage, which demonstrates that multilayers of HRP entrapped in the ss-DNA/GP matrix participated in the electron-transfer process. Reasons for the multilayer electron-transfer process are possibly the conductivity, the biocompability of the ss-DNA/GP nanocomposite, and the favorable orientation of the immobilized HRP.

Electrocatalytic properties of the HRP/ss-DNA/GP/GC electrode for H_2O_2 reduction: Hydrogen peroxide (H_2O_2) is an essential mediator in biology, medicine, industry, and many other fields, and the sensitive and accurate determination of H_2O_2 is therefore of great importance.[30] The electrocatalytic reduction of H_2O_2 at the ss-DNA/GP/GC and HRP/ss-DNA/GP/GC electrodes were studied by cyclic voltammetry. No peak was observed in the CVs of the ss-DNA/GP/GC electrode in the presence of H_2O_2 within the potential range of 0.2 to −0.8 V, which suggested that the ss-DNA/GP/GC electrode was inactive to direct reduction of H_2O_2. However, an obvious increase of the reduction peak current was observed at the HRP/ss-DNA/GP/GC electrode when H_2O_2 was added to the PBS, accompanied by a decrease of the oxidation peak current (Figure 6A; the figure is elided to the potential range of 0.2 to −0.8 V). This demonstrates a typical electrocatalytic process of H_2O_2 by HRP immobilized in the ss-DNA/GP matrix.

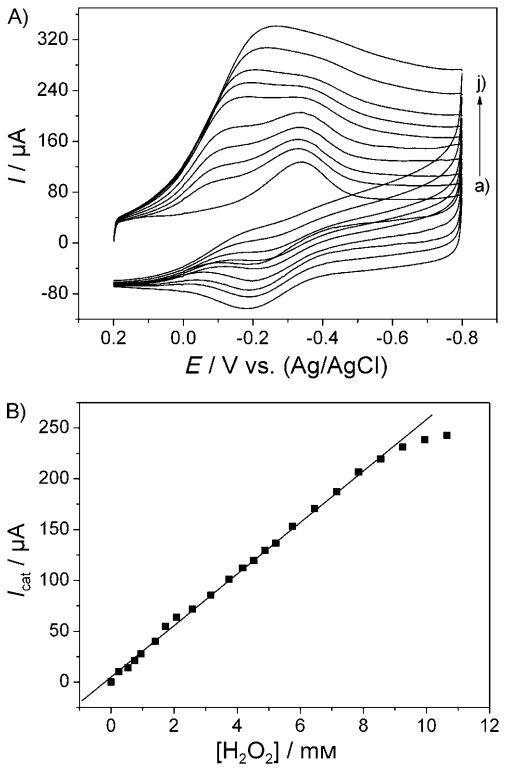

Figure 6. A) Cyclic voltammograms of the HRP/ss-DNA/GP/GC electrode in 0.1 M PBS (pH 7.0) with a) 0, b) 0.745, c) 1.165, d) 1.725, e) 2.425, f) 3.825, g) 4.525, h) 5.225, i) 6.45, and j) 7.85 mM H_2O_2. B) Plot of the electrocatalytic current (I_{cat}) versus H_2O_2 concentration for the HRP/ss-DNA/GP/GC electrode. Scan rate: 200 mV s^{-1}.

The electrocatalytic process of H_2O_2 by HRP can be described by Equations (1)–(5).[31]

$$\mathrm{HRP[Heme(Fe^{III})] + H_2O_2 \rightarrow Compound\ \mathbf{1} + H_2O} \quad (1)$$

$$\mathrm{Compound\ \mathbf{1} + H_2O_2 \rightarrow HRP[Heme(Fe^{III})] + H_2O + O_2} \quad (2)$$

$$\mathrm{HRP[Heme(Fe^{III})] + H^+ + e^- \rightarrow HRP[Heme(Fe^{II})]\ (at\ electrode)} \quad (3)$$

$$\mathrm{HRP[Heme(Fe^{II})] + O_2 \rightarrow HRP[Heme(Fe^{II})] - O_2\ (fast)} \quad (4)$$

$$\mathrm{HRP[Heme(Fe^{II})] - O_2 + H^+ + e^- \rightarrow HRP[Heme(Fe^{III})] + H_2O_2\ (at\ electrode)} \quad (5)$$

As shown in Figure 6A, two reduction peaks could be observed at −0.13 and −0.31 V. These two reduction peaks are the reduction peaks of O_2 and HRP[Heme(Fe^{III})] at the HRP/ss-DNA/GP/GC electrode, respectively; these are consistent with the electrode reactions described in Equations (3) and (5). When H_2O_2 was added to the PBS, HRP-[Heme(Fe^{III})] and O_2 could be formed according to Equations (1) and (2); thus, the reduction peaks at −0.13 and −0.31 V increased upon an increase in the H_2O_2 concentration. Once the concentration of H_2O_2 reached a high level, it could be observed that these two reduction peaks overlapped and integrated into one reduction peak.[32] The linear relationship between the electrocatalytic current (I_{cat}) and the concentration of H_2O_2 is shown in Figure 6B. It can be observed that the cathodic peak currents increased linearly with concentrations of H_2O_2 from 115.5 μM to 9.25 mM. The linear range of the HRP/ss-DNA/GP/GC electrode was much wider than most of the reported values for other biocompatible nanocomposite electrodes.[16,22,23,25] The reason for the wide linear range was possibly the well-retained bioactivity of the HRP immobilized on the conductive and biocompatible ss-DNA/GP nanocomposite. The detection limit for the biosensor was 38.5 μM, based on a signal/noise ratio of 3, and its linear regression equation was $y=25.33x+4.98$ ($R=0.9989$, $n=21$), in which y and x stand for the peak current (in μA) and the concentration (in mM) of H_2O_2, respectively. From the slope of the line, the sensitivity of the HRP/ss-DNA/GP/GC electrode was calculated to be 356.6 $mA\,cm^{-2}\,M^{-1}$, which was also higher than the previously reported HRP-based modified electrode.[29] The high sensitivity suggested that the immobilized HRP on the ss-DNA/GP matrix had good bioelectrocatalytic activity for H_2O_2.

Reproducibility and stability of the HRP/ss-DNA/GP/GC electrode: The reproducibility and stability of the HRP/ss-DNA/GP/GC electrode were also studied. The relative standard deviation (RSD) is 3.2% for 6 successive measurements of 200 μM H_2O_2 in 0.1 M PBS (pH 7.0), which indicated that the modified electrode possessed good reproducibility. To investigate the stability of the HRP/ss-DNA/GP/GC electrode, the modified electrode was stored continuously in pH 7.0 buffer at 4°C and CVs were measured after a period of storage time. The decrease in the cathodic peak current was negligible after 12 h, which demonstrated that the HRP/ss-DNA/GP/GC electrode was stable in buffer solution. The long-term stability of the HRP/ss-DNA/GP/GC electrode was also tested. After the modified electrode had been stored at 4°C for a week, the currents for the direct electron transfer of HRP and the responses to 200 μM H_2O_2 had not changed. Even after storage for a month, the reduction current of H_2O_2 still remained at 95% of its initial value. These results indicated that the HRP/ss-DNA/GP/GC electrode had a good stability toward the electrocatalytic reduction of H_2O_2; this stability could be attributed to the good film-forming ability and excellent biocompatibility of the ss-DNA/GP nanocomposite.

Conclusion

A novel HRP/ss-DNA/GP/GC electrode was constructed through self-assembly between HRP and an ss-DNA/GP nanocomposite on the surface of a GC electrode. FTIR and UV/Vis spectra were utilized to monitor the assembly process. The spectral results also demonstrated that HRP was immobilized onto the ss-DNA/GP nanocomposite without denaturation. The experimental results indicated that the biocompatible matrix supplied a necessary pathway for the immobilized HRP to achieve direct electrochemistry. Furthermore, the HRP/ss-DNA/GP/GC electrode performed good electrocatalytic reduction for H_2O_2 with good sensitivity, good stability, and a wide linear range. Therefore, such a multicomponent platform, which integrates the advantages of GP, DNA, and the redox enzyme together, may have promising potential for the fabrication of mediator-free biosensors or bioreactors.

Experimental Section

Materials: Native double-stranded DNA (ds-DNA) from calf thymus and horseradish peroxide (HRP; molecular weight = 44 kDa) were purchased from Sigma Chemical (USA). Graphite powder (99.95%, 325 mesh), hydrogen peroxide solution (30 wt% aqueous), and hydrazine solution (50 wt%) were purchased from the Shenyang Chemical Company and used as received. All solutions were prepared by using Milli-Q purified water (> 18.0 $M\Omega\,cm^{-1}$).

Preparation of graphite oxide: GO was prepared from graphite powder according to the method of Hummers and Offeman.[20] Briefly, powered flake graphite (2 g) and $NaNO_3$ (1.6 g) were added to 98% H_2SO_4 (67.5 mL) in an ice bath. After that, $KMnO_4$ (9 g) was slowly added to the mixture with stirring. The mixture was then maintained at 35°C for 30 min. After the mixture had been kept at room temperature with mechanical stirring for 5 days, warm water (560 mL) was slowly stirred into the paste and it was then further treated with 30% H_2O_2 (4 mL). Upon treatment with the peroxide, the suspension turned bright yellow. The suspension was then centrifuged, washed with distilled water, and air dried overnight at 70°C to obtain GO.

Preparation of unmodified GP and the ss-DNA/GP nanocomposite: To synthesize unmodified GP, hydrazine (0.4 mL, 85 wt%) was added to a dispersion of GO (10 mL, 2.5 $mg\,mL^{-1}$) and the mixture was heated to reflux for 3 h. The mixture was then centrifuged and washed with distilled water three times to remove excess hydrazine.

The ss-DNA/GP nanocomposite was synthesized according to the reported method with a slight modification.[19] Briefly, an aqueous solution of ds-DNA (6 $mg\,mL^{-1}$) was first heated at 95°C for 2 h to obtain an aqueous solution of ss-DNA. GO (100 mg) was dispersed in water (40 mL), and the mixture was sonicated for 3 h to get a homogeneous yellow-brown dispersion. The GO dispersion (10 mL, 2.5 $mg\,mL^{-1}$) was then mixed with the aqueous solution of ss-DNA (20 mL, 6 $mg\,mL^{-1}$), and the resultant mixture was stirred for 0.5 h. Subsequently, hydrazine (0.4 mL, 85 wt%) was added to the mixture. The mixture was then heated to reflux at 100°C for 4 h to prepare the ss-DNA/GP nanocomposite. After cooling to room temperature, the resulting materials were then centrifuged and washed three times with distilled water to remove excess hydrazine and ss-DNA. The as-prepared ss-DNA/GP nanocomposite was water soluble and could be stored as an aqueous solution at a concentration of 1 $mg\,mL^{-1}$.

Preparation of the HRP/ss-DNA/GP/GC electrode: Prior to use, a glassy carbon electrode with a diameter of 3 mm was polished on a polishing cloth with 1.0, 0.3, and 0.05 μm alumina powder and rinsed with deion-

ized water, before it was subjected to sonication in acetone, ethanol, and deionized water successively. The electrode was then allowed to dry at room temperature. To prepare the HRP/ss-DNA/GP/GC electrode, an aqueous dispersion of ss-DNA/GP (5 μL, 1 mg mL^{-1}) was cast onto the GC electrode. A beaker was placed over the electrode so that the water could evaporate slowly in air and a uniform film electrode could be formed. The ss-DNA/GP modified electrode was then immersed in 0.10 M phosphate buffer solution (pH 5.0) containing HRP (4 mg mL^{-1}) for 24 h to construct the HRP/ss-DNA/GP/GC electrode (Figure 1). The as-prepared HRP/ss-DNA/GP/GC electrode was rinsed with deionized water and stored at 4 °C in a refrigerator when not in use.

For comparison with the HRP/ss-DNA/GP/GC electrode, ss-DNA/GP/GC and HRP/GC electrodes were prepared with the same procedures as those described above. A solution containing ss-DNA/GP nanocomposite (1 mg mL^{-1}) was used to prepare the ss-DNA/GP/GC electrode, and another solution containing HRP (4 mg mL^{-1}) was used to prepare the HRP/GC electrode.

Apparatus and measurements: Electrochemical measurements were performed at room temperature by using a BAS100B workstation (Bioanalytical Systems Inc., USA). The measurements were based on a three-electrode system with the as-prepared modified electrode as the working electrode, a platinum wire as the counter electrode, and a saturated Ag/AgCl electrode as the reference electrode. Unless otherwise noted, 0.1 M phosphate buffer solution (pH 7.0) was used as the electrolyte solution in all experiments. The buffer solution was purged with highly purified nitrogen for at least 30 min, and a nitrogen atmosphere was maintained throughout the electrochemical measurements.

UV/Vis experiments were performed with a UV-2100S spectrophotometer (Shimadzu). The FTIR spectra of samples in KBr pellets were recorded on a PerkinElmer FT 1730 instrument. The morphology of the ss-DNA/GP nanocomposite was observed by utilizing a Hitachi model H-800 transmission electron microscope opened at an accelerating voltage of 100 kV. The zeta-potential data of the ss-DNA/GP nanocomposite and the ss-DNA were obtained by using a Zeta-Plus4 instrument (Brookhaven Corp., USA).

Acknowledgements

This work was financially supported by the National Natural Science Foundation of China (20671046, 20975060, and 20901035), the National Basic Research Program of China (2007CB310500), and the Natural Science Foundation of Liaoning Province (20072053, 2006T070, 2005L158, 2009B169, and 2009T041).

[1] a) J. H. Zhou, X. B. Lu, J. Q. Hu, J. H. Li, *Chem. Eur. J.* **2007**, *13*, 2847–2853; b) X. B. Lu, J. Q. Hu, X. Yao, Z. P. Wang, J. H. Li, *Biomacromolecules* **2006**, *7*, 975–980.

[2] a) C. W. Ge, M. Xu, J. H. Fang, J. P. Lei, H. X. Ju, *J. Phys. Chem. C* **2008**, *112*, 10602–10608; b) R. J. Cui, C. Liu, J. M. Shen, D. Gao, J. J. Zhu, H. Y. Chen, *Adv. Funct. Mater.* **2008**, *18*, 2197–2204.

[3] Y. Zhou, H. Yang, H. Y. Chen, *Talanta* **2008**, *76*, 419–423.

[4] a) Y. Wang, J. Lu, L. Tang, H. X. Chang, J. H. Li, *Anal. Chem.* **2009**, *81*, 9710–9715; b) Y. M. Li, L. H. Tang, J. H. Li, *Electrochem. Commun.* **2009**, *11*, 846–849; c) C. N. R. Rao, K. Biswas, K. S. Subrahmanyama, A. Govindaraj, *J. Mater. Chem.* **2009**, *19*, 2457–2469.

[5] a) A. Ghosh, K. V. Rao, S. J. George, C. N. R. Rao, *Chem. Eur. J.* **2010**, *16*, 2700–2704; b) W. J. Hong, Y. X. Xu, G. W. Lu, C. Li, G. Q. Shi, *Electrochem. Commun.* **2008**, *10*, 1555–1558; c) J. L. Vickery, A. J. Patil, S. Mann, *Adv. Mater.* **2009**, *21*, 2180–2184; d) L. H. Tang, Y. Wang, Y. M. Li, H. B. Feng, J. Lu, J. H. Li, *Adv. Funct. Mater.* **2009**, *19*, 1–8.

[6] a) M. Zhou, Y. M. Zhai, S. J. Dong, *Anal. Chem.* **2009**, *81*, 5603–5613; b) X. H. Kang, J. Wang, H. Wu, I. A. Aksay, J. Liu, Y. H. Lin, *Biosens. Bioelectron.* **2009**, *25*, 901–905; c) Y. Wang, Y. M. Li, L. H. Tang, J. Lu, J. H. Li, *Electrochem. Commun.* **2009**, *11*, 889–892.

[7] a) S. Alwarappan, A. Erdem, C. Liu, C. Z. Li, *J. Phys. Chem. C* **2009**, *113*, 8853–8857; b) X. Chen, C. L. Fu, W. S. Yang, *Analyst* **2009**, *134*, 2135–2140.

[8] C. S. Shan, H. F. Yang, J. F. Song, D. X. Han, A. Ivaska, L. Niu, *Anal. Chem.* **2009**, *81*, 2378–2382.

[9] Y. Wang, W. S. Yang, C. Chen, D. G. Evans, *Electrochem. Commun.* **2008**, *10*, 1264–1267.

[10] S. M. Chen, S. V. Chen, *Electrochim. Acta* **2003**, *48*, 513–529.

[11] N. W. S. Kam, Z. Liu, H. J. Dai, *J. Am. Chem. Soc.* **2005**, *127*, 12492–12493.

[12] E. L. Gui, L. J. Li, K. Zhang, Y. P. Xu, X. C. Dong, X. N. Ho, P. S. Lee, J. Kasim, Z. X. Shen, J. A. Rogers, S. G. Mhaisalkar, *J. Am. Chem. Soc.* **2007**, *129*, 14427–14432.

[13] B. S. Harrison, A. Atala, *Biomaterials* **2007**, *28*, 344–353.

[14] J. W. Shie, U. Yogeswaran, S. M. Chen, *Talanta* **2008**, *74*, 1659–1669.

[15] A. Bhambhani, C. V. Kumar, *Adv. Mater.* **2006**, *18*, 939–942.

[16] X. D. Zeng, X. F. Li, X. Y. Liu, Y. Liu, S. L. Luo, B. Kong, S. L. Yang, W. Z. Wei, *Biosens. Bioelectron.* **2009**, *25*, 896–900.

[17] Q. Zhang, L. Zhang, J. H. Li, *J. Phys. Chem. C* **2007**, *111*, 8655–8660.

[18] a) N. Varghese, U. Mogera, A. Govindaraj, A. Das, P. K. Maiti, A. K. Sood, C. N. R. Rao, *ChemPhysChem* **2009**, *10*, 206–210; b) C. H. Lu, H. H. Yang, C. L. Zhu, X. Chen, G. N. Chen, *Angew. Chem.* **2009**, *121*, 4879–4881; *Angew. Chem. Int. Ed.* **2009**, *48*, 4785–4787.

[19] J. Patil, J. L. Vickery, T. B. Scott, S. Mann, *Adv. Mater.* **2009**, *21*, 1–6.

[20] W. S. Hummers, Jr., R. E. Offeman, *J. Am. Chem. Soc.* **1958**, *80*, 1339.

[21] S. Vadukumpully, J. Paul, S. Valiyaveettil, *Carbon* **2009**, *47*, 3288–3294.

[22] X. H. Chen, C. M. Ruan, J. Kong, J. Q. Deng, *Anal. Chim. Acta* **2000**, *412*, 89–98.

[23] L. Zhang, Q. Zhang, X. B. Lu, J. H. Li, *Biosens. Bioelectron.* **2007**, *23*, 102–106.

[24] X. B. Lu, Z. H. Wen, J. H. Li, *Biomaterials* **2006**, *27*, 5740–5747.

[25] S. F. Wang, F. Xie, G. D. Liu, *Talanta* **2009**, *77*, 1343–1350.

[26] D. M. Sun, C. X. Cai, X. G. Li, W. Xing, T. H. Lu, *J. Electroanal. Chem.* **2004**, *566*, 415–421.

[27] H. S. Yin, S. Y. Ai, W. J. Shi, L. S. Zhu, *Sens. Actuators B* **2009**, *137*, 747–753.

[28] K. P. Liu, J. J. Zhang, G. H. Yang, C. M. Wang, J. J. Zhu, *Electrochem. Commun.* **2010**, *12*, 402–405.

[29] X. B. Lu, Q. Zhang, L. Zhang, J. H. Li, *Electrochem. Commun.* **2006**, *8*, 874–878.

[30] W. Sun, X. Q. Li, K. Jiao, *Electroanalysis* **2009**, *21*, 959–964.

[31] H. Huang, N. F. Hu, Y. H. Zeng, G. Zhou, *Anal. Biochem.* **2002**, *308*, 141–151.

[32] X. B. Lu, H. Zhang, Y. W. Ni, Q. Zhang, J. P. Chen, *Biosens. Bioelectron.* **2008**, *24*, 93–98.

Received: March 18, 2010
Published online: June 25, 2010

